Stability of rays traveling through Gaussian random potential

Elizabeth Bernhardt

July 2009

Abstract

We present an exploration of the stability of long-range propagation through random media. As a ray travels through a medium, it encounters variations which cause slight changes in velocity. Sound in the ocean, for example, propagates through varying temperature and salination. Over long ranges, these variations cause the ray to become chaotic. In order to determine the behavior of the ray, the evolution of its stability matrix must be studied. Through creation of an adaptive step-size Runge-Kutta differential equations solver, we examined the stability matrices of several hundred rays to determine the transition with increaing propagation time between stable propagation and chaos. Our findings suggest the timing of the transition is dependent on the initial kinetic energy in proportion to the average maxima and minima of the randomized plane potential. We would like to understand if rays with larger intial momentum tend to chaos as fast as rays with lower initial momentum. Our results relate to our understanding of the phenomenon of coherent branching of electron flow through quantum point contacts (Ref. [3]) and long range acoustic propagation through the ocean (Ref. [1]) as well as other physical contexts.

1 INTRODUCTION

The study done by Wolfson and Tomsovic in Ref. [4] investigated sound traveling in the ocean using classical rays. They found that the rays tends to become chaotic due to sound speed variations due to temperature and salination. As the sound propagates further from its source, these variations cause the sound rays to become chaotic. They argue that the stability exponents characterizing the chaos should follow a log-normal distribution and demonstrate this to good agreement for all but the tails of the distribution. A log-normal distribution has long tails implying stable rays with small exponents will exist at all ranges yet it is known that the rays become chaotic after a certain range, the predictability horizon.

This study attempts to discover a better model for the distribution of the stability exponents times close to the predictability horizon. Ray simulations through a Gaussian random potential with zero-mean and unit variance are done for a large number of rays and the distribution of the stability exponents is found. Using Fortran, we coded a program to send rays through the randomized potential. Utilizing fourth order Runge-Kutta techniques, we found the solution to several differential equations which govern our system including ray location and stability matrix components.

2 MODEL

The energy of a classical ray at location (x, y) is described by the classical Hamiltonian

$$H(x, y) = (p_x^2 + p_y^2)/2m + V(x, y) \tag{1}$$

where $V(x, y)$ is the potential energy at said location, p_x and p_y are the momenta in the x and y directions, and m is the mass. Without overgeneralization, m is taken to be 1. Further, the total momentum $p_{tot} = \sqrt{p_x^2 + p_y^2}$.

2.1 Classical Propagation

Classical rays with the Hamiltonian in Eq. (1) propagate according to Hamilton's Equations simplified to

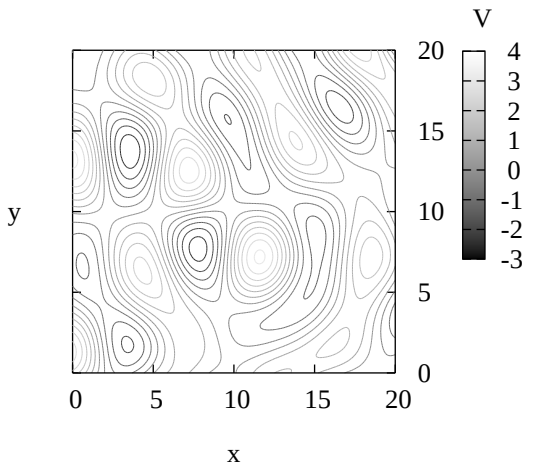

Figure 1: A contour plot of the Gaussian random potential function $V(x, y)$ in Eq. (3) with scale length L as a function locations x' and y' in units of $L/2\pi$.

$$\begin{aligned} \frac{dx}{dt} &= p_x \\ \frac{dy}{dt} &= p_y \\ \frac{dp_x}{dt} &= -\frac{\partial V(x,y)}{\partial x} \\ \frac{dp_y}{dt} &= -\frac{\partial V(x,y)}{\partial x} \end{aligned} \tag{2}$$

where x and y are the location of the ray, p_x and p_y are the momenta of the ray in the x and y directions, and $V(x, y)$ is the potential function. The trajectory of the ray is defined by $(x(t), y(t), p_x(t), p_y(t))$. Note that the Hamiltonian is not explicitly dependent on time t, so the energy of each ray is conserved as it propagates. The energy simply sloshes between kinetic and potential energy.

2.2 Potential

The desired potential for this study is a Gaussian random field with zero-mean and unit variance. To achieve this, the potential function $V(x, y)$ is created from a superposition of N random plane waves with random direction θ_j, random phase ϕ_j, and constant wavelength L. This section describes the construction of this potential and verifies it has the appropriate properties.

Consider a single plane wave with wavenumber $k = 2\pi/L$, where L is wavelength oriented at an angle θ counter clockwise from x' axis with wavevector $\vec{k} = (k\cos\theta, k\sin\theta)$. Let the phase at (0,0) be ϕ_j. Then the potential at $\vec{x}' = (x', y')$ is

$$V(x', y') = Re\left[\frac{e^{i(\vec{k}\cdot\vec{x}'+\phi_j)}}{\sqrt{2\pi L}}\right] = \frac{1}{\sqrt{2\pi L}}\cos(kx'\cos\theta_j + ky'\sin\theta_j + \phi_j).$$

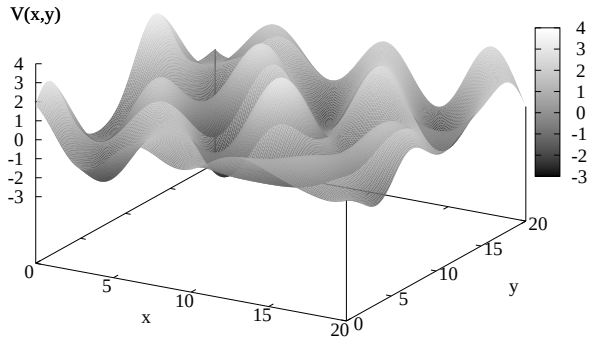

Figure 2: The Gaussian random potential in Eq. (3) is plotted at locations x and y which are dimensionless variables in units of $L/2\pi$.

Now consider the superposition of N such plane waves with random angle θ_j, random phase ϕ_j, and each with the same wavelength L to create the potential

$$V(x',y') \quad = \quad \frac{1}{\sqrt{2\pi L}} \sum_{j=1}^{N} \cos(kx' \cos\theta_j + ky' \sin\theta_j + \phi_j)$$

where the random variables θ_j and ϕ_j are both uniform distributed on [0,2π]. Dimensionless variables allow for our model to be applicable on any scale or situation, such as the ocean of Ref. [4] or the electrons of Ref. [3]. Therefore, let $x = kx'$, $y = ky'$ where $k = 2\pi/L$. Then the potential in dimensionles variables (x,y) takes the form

$$V(x,y) \quad = \quad \frac{1}{\sqrt{2\pi L}} \sum_{j=1}^{N} \cos(x \cos\theta_j + y \sin\theta_j + \phi_j)$$

If N is sufficently large then V is a large sum of random variables and by the central limit theorem, V is Gaussian. Let $X_j = \frac{1}{\sqrt{2\pi L}} \cos(x \cos\theta_j + y \sin\theta_j + \phi_j)$ and $\langle\cdot\rangle$ denote averaging of a quantity over all the random variables. Then

$$\langle V \rangle \quad = \quad \sum_{j=1}^{N} \langle X_j \rangle$$

and

$$\sigma_V^2 = \langle (V - \langle V \rangle)^2 \rangle = \langle V^2 \rangle - \langle V \rangle^2 = \sum_{j=1}^{N} \langle X_j^2 \rangle - \langle X_j \rangle^2.$$

The potential V needs to have zero-mean. Note that since $\theta, \phi \in U[0, 2\pi]$ their probability distribution functions are $f(\theta) = 1/2\pi$ and $f(\phi) = 1/2\pi$ and

$$\langle X_j \rangle \quad = \quad \int_0^{2\pi} d\theta \int_0^{2\pi} d\phi X(\theta,\phi) f_1(\theta) f_2(\phi)$$

$$
\begin{aligned}
&= \int_0^{2\pi} \frac{d\theta}{2\pi} \int_0^{2\pi} \frac{d\phi}{2\pi} \frac{1}{2\pi} \cos(x\cos\theta + y\sin\theta + \phi) \\
&= Re\left[\int_0^{2\pi} \frac{d\theta}{2\pi} \int_0^{2\pi} \frac{d\phi}{2\pi} e^{i(x\cos\theta + y\sin\theta + \phi)}\right] \\
&= Re\left[\int_0^{2\pi} \frac{d\theta}{2\pi} e^{i(x\cos\theta + y\sin\theta)} \int_0^{2\pi} \frac{d\phi}{2\pi} e^{i\phi}\right] \\
&= 0
\end{aligned}
$$

where the integral has been transformed using Euler's formula and separation of θ, ϕ integrals and finally, $\int_0^{2\pi} \frac{d\phi}{2\pi} e^{i\phi} = 0$.

The potential must also have unit variance. Since $\langle X_j \rangle = 0$, $\sigma_X^2 = \langle X^2 \rangle$ and

$$
\begin{aligned}
\langle X_j^2 \rangle &= \int_0^{2\pi} \int_0^{2\pi} \frac{d\theta}{2\pi} \frac{d\phi}{2\pi} \frac{\cos^2(x\cos\theta + y\sin\theta + \phi)}{2\pi L} \\
&= \frac{1}{2\pi L} \int_0^{2\pi} \frac{d\theta}{2\pi} \int_0^{2\pi} \frac{d\phi}{2\pi} \left(\frac{1}{2} + \frac{1}{2}\cos\left(2\left(x\cos\theta + y\sin\theta + \phi\right)\right)\right) \\
&= \frac{1}{2\pi L} \int_0^{2\pi} \int_0^{2\pi} \frac{d\theta d\phi}{(2\pi)^2} \frac{1}{2} + \frac{1}{2} \frac{1}{2\pi L} Re\left[\int_0^{2\pi} \frac{d\theta}{2\pi} e^{i(2x\cos\theta + 2y\sin\theta)} \int_0^{2\pi} \frac{d\phi}{2\pi} e^{2i\phi}\right] \\
&= \frac{1}{2\pi L} \int_0^{2\pi} \int_0^{2\pi} \frac{d\theta d\phi}{(2\pi)^2} \frac{1}{2} \\
&= \frac{1}{2} \frac{1}{2\pi L}
\end{aligned}
$$

Since

$$
\sigma_V^2 = \sum_{j=1}^{N} \langle X_j^2 \rangle = \sum_{j=0}^{N} \frac{1}{4\pi L} = \frac{N}{4\pi L}
$$

and we want $\sigma_V^2 = 1$. Let the normalization potential be $V' = cV$ and let c=$1/\sqrt{\sigma_V^2}$. So we normalize V using

$$
V' = \frac{V}{\sqrt{\frac{N}{2}\frac{1}{2\pi L}}}
$$

so that

$$
\sigma_{V'}^2 = \frac{\sigma_V^2}{\frac{N}{2}} = \frac{\frac{N}{2}\frac{1}{2\pi l}}{\frac{N}{2}\frac{1}{2\pi l}} = 1.
$$

So our normalized potential function in dimensionless variables (x,y) is

$$
V(x,y) = \sqrt{\frac{2}{N}} \sum_{j=1}^{N} \cos\left(x\cos\theta_j + y\sin\theta_j + \phi_j\right). \tag{3}
$$

As demonstrated, this potential satisfies zero-mean and unit variance and in taking N=10000, the central limit theorem grants that our potential is a Gaussian distribution. See appendix B for a discussion of programming pseudo-random variables. Contours and a 3D graph of the potential in Eq. (3) are illustrated in Fig. 1 and 2.

2.3 Stability Matrices

One of the key tools of our investigation is the stability matrix M where

$$M = \begin{pmatrix} m_{11} & m_{12} & m_{13} & m_{14} \\ m_{21} & m_{22} & m_{23} & m_{24} \\ m_{31} & m_{32} & m_{33} & m_{34} \\ m_{41} & m_{42} & m_{43} & m_{44} \end{pmatrix} = \begin{pmatrix} \frac{\partial p_x}{\partial p_{x_0}}|_{x_0,y_0} & \frac{\partial p_y}{\partial p_{x_0}}|_{x_0,y_0} & \frac{\partial p_x}{\partial x_0}|_{p_{x_0},p_{y_0}} & \frac{\partial p_y}{\partial x_0}|_{p_{x_0},p_{y_0}} \\ \frac{\partial p_x}{\partial p_{y_0}}|_{x_0,y_0} & \frac{\partial p_y}{\partial p_{y_0}}|_{x_0,y_0} & \frac{\partial p_x}{\partial y_0}|_{p_{x_0},p_{y_0}} & \frac{\partial p_y}{\partial y_0}|_{p_{x_0},p_{y_0}} \\ \frac{\partial x}{\partial p_{x_0}}|_{x_0,y_0} & \frac{\partial y}{\partial p_{x_0}}|_{x_0,y_0} & \frac{\partial x}{\partial x_0}|_{p_{x_0},p_{y_0}} & \frac{\partial y}{\partial x_0}|_{p_{x_0},p_{y_0}} \\ \frac{\partial x}{\partial p_{y_0}}|_{x_0,y_0} & \frac{\partial y}{\partial p_{y_0}}|_{x_0,y_0} & \frac{\partial x}{\partial y_0}|_{p_{x_0},p_{y_0}} & \frac{\partial y}{\partial y_0}|_{p_{x_0},p_{y_0}} \end{pmatrix}. \quad (4)$$

This matrix describes the dynamical behavior of rays that propagate infinitesmally close to a given ray r with initial conditions $(x_0, y_0, p_{x_0}, p_{y_0})$. Stable propagation means that all the rays with initial conditions in an infinitely small neighborhood $\{\delta x, \delta y\}$ about $(x_0, y_0, p_{x_0}, p_{y_0})$ move elliptically around r. These neighboring rays follow the path of r after small perturbations away from r. Chaotic propagation is marked by exponential movement away from r after a small perturbation.

For a system with one degree of freedom, such as the ocean in Ref. [4], it is easily apparent whether the ray is stable or unstable based on the trace $\mathrm{Tr}(M)$ of the matrix. If $|Tr(M)|$ is less than 2, the ray is stable, else it is unstable. For a system with two degrees of freedom, there is no clear cut boundary between stability and chaos. Instead, the evolution of the matrix aids in determining the type of propagation of a ray. As the ray propagates, the matrix evolves according to

$$\frac{d}{dt}M = KM \quad (5)$$

where

$$K = \begin{pmatrix} 0 & 0 & -\frac{\delta^2 V(x,y)}{\delta x^2} & -\frac{\delta^2 V(x,y)}{\delta x \delta y} \\ 0 & 0 & -\frac{\delta^2 V(x,y)}{\delta y \delta x} & -\frac{\delta^2 V(x,y)}{\delta^2 y} \\ 1 & 0 & 0 & 0 \\ 0 & 1 & 0 & 0 \end{pmatrix} \quad (6)$$

with initial condition $M = I$, where I is the identity matrix.

The trace of the stability matrix $\mathrm{Tr}(M)$ is calculated by summing the entries on the diagonal,

$$Tr(M) = \sum_{i=1}^{4} m_{ii}.$$

$\mathrm{Tr}(M)$ changes through time. Furthermore, the stability matrix M can be diagonalized by the similarity transform $M = L^{-1}\Lambda L$ where Λ contains the eigenvalues λ of M,

$$\Lambda = \begin{pmatrix} \lambda_1 & 0 & 0 & 0 \\ 0 & \lambda_2 & 0 & 0 \\ 0 & 0 & \lambda_3 & 0 \\ 0 & 0 & 0 & \lambda_4 \end{pmatrix}.$$

Since this transformation does not change the trace of the matrix M,

$$Tr(M) = Tr(L^{-1}\Lambda L) = \frac{1}{Tr(L)}Tr(\Lambda)Tr(L) = Tr(\Lambda) = \lambda_1 + \lambda_2 + \lambda_3 + \lambda_4. \quad (7)$$

The eigenvalues λ_i can be real or complex numbers; since $\mathrm{Tr}(M)$ is a real number complex eigenvalues come in conjugate pairs.

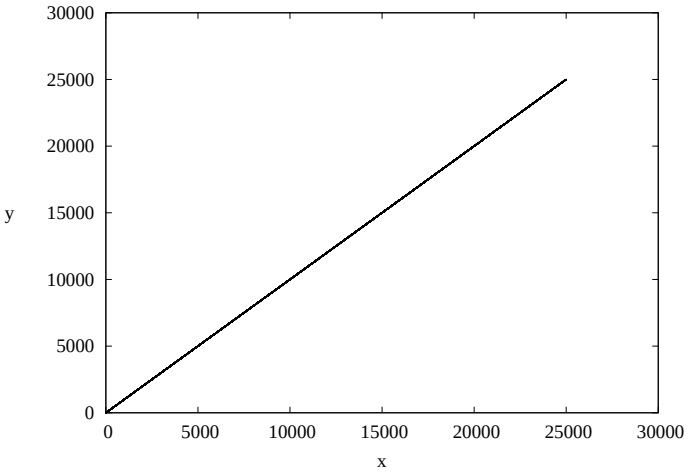

Figure 3: One hundred rays propagated to time $t = 25$ with $p_{x_0} = p_{y_0} = 1000$ and $y_0 = 0$ with $\delta y = 0.01$ The trajectories are plotted as a function of x, y in units of $L/2\pi$. Note that due to their high kinetic energy they propagate in a stable bundle and cannot be distinguished from each other in the plot.

2.4 Stability and Lyapunov Exponents

Infinitely close rays separate by a factor of $\lambda = e^{\nu t}$ with ν being the stability exponent. As the ray propagates, its stability is determined by ν where

$$\nu = \frac{\ln |Tr(M)|}{t}. \tag{8}$$

The stability exponent evolves through time t and is dependent on one ray only. It describes the stability of a particular ray at time t. The Lyapunov exponent ν_L, on the other hand, is

$$\nu_L = \lim_{t\to\infty} \frac{\ln |Tr(M)|}{t}. \tag{9}$$

As $t \to \infty$ Tr(M) is dominated by one eigenvalue $\lambda = max\{\lambda_i\}$. The Lyapunov exponent differs from the stability exponent in that it is ray independent and independent of the particular realization of the potential (see Ref. [4]). Thus, all the stability exponents ν_i converge to ν_L.

3 Numerical Simulations

In order to find the distribution of the stability exponent ν, we ran 100 rays at a time through the potential in Eq. (3). We peformed several of these runs and changed only the intial x-location for each individual run. Each ray was given the same intial momenta p_{x_0} and p_{y_0} and the same initial x-location x_0. The y-location was varied by $\delta y = 0.01$ for each ray. The rays were allowed to propagate to a user defined time t.

3.1 Ray Propagation

Rays are extremely sensitive to initial conditions; this causes an exponential growth of separation of nearby rays. The kinetic energy of a ray is $p_{tot}^2/2$. At short ranges, the initial momenta determine how quickly the rays fan out and become chaotic. Rays with kinetic energy less than V_{rms} tend to be reflected by the potential and are not of interest to us. In Fig. 4 ten rays were propagated for a short time to demonstrate what happens to rays with low initial kinetic energy. However, rays with kinetic energy greater than V_{rms} are of interest. Their transition to chaotic propagation is not well defined. Indeed, the rays in Fig. 3 have such a high initial kinetic energy that at time $t = 50$ they are still propagating together.

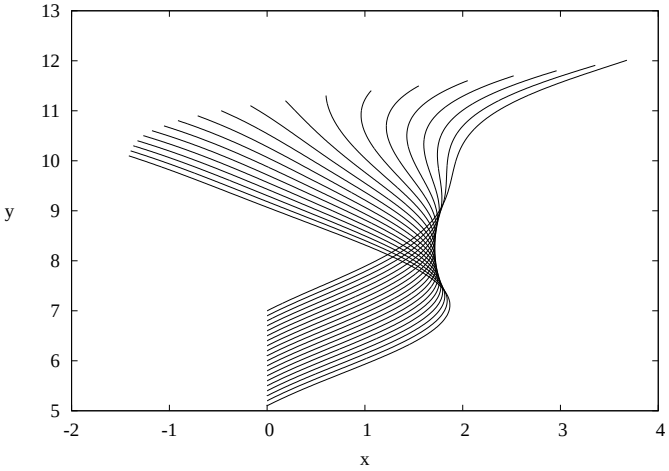

Figure 4: Twenty rays propagated to time $t = 10$ with $p_{x_0} = p_{y_0} = 1$ and $y_0 = 5$ with $\delta y = 0.1$. Although these rays have not yet begun exponentially propagating away from each other, they soon will. Note that these rays propagate parallel to each other until they reflect from the potential and diverge form each other. The kinetic energy of these rays is less than V_{rms}.

When the initial momenta are large values, such as 1000, the rays tend to be stable for longer times. Meanwhile, small initial kinetic energies, such as 1 or 3, tend to chaos much sooner. This is because the ray with a large kinetic energy does not feel the changes in potential as much as the ray with a smaller kinetic energy. This is much like a car traveling on a bumpy highway, the faster the car travels, the smoother the road seems.

3.2 Linear Regression and Stability Exponent

In order to establish the difference between stable propagation and chaotic propagation, we need a way to distinguish between algebraic growth and exponential growth of $\mathrm{Tr}(M)$. A good model for the time evolution of $\mathrm{Tr}(M)$ is given in Ref. [2] as

$$|Tr(M)| \sim t^{\mu} e^{\alpha+\nu t} \tag{10}$$

where t is time, α and μ are constants describing stable propagation, and ν is an approximation of the stability exponent. Since the model $\ln|Tr(M)| \sim \alpha + \nu t + \mu \ln(t)$ is linear, a least square regression can be used to minimize the integral

$$\int_{t_{min}}^{t} ds \left(\ln|Tr(M)| - \alpha - \mu \ln s - \nu s\right)^2 . \tag{11}$$

This can be solved using ratio of determinants:

$$\hat{\beta} = \left(X^T X\right)^{-1} X^T \vec{y} \tag{12}$$

where $(\cdot)^T$ signifies transpose of a matrix, $(\cdot)^{-1}$ signifies matrix inverse and

$$X = \begin{pmatrix} 1 & t_1 & \ln t_1 \\ 1 & t_2 & \ln t_2 \\ & \cdots & \\ 1 & t_N & \ln t_N \end{pmatrix}; \hat{\beta} = \begin{pmatrix} \alpha \\ \nu \\ \mu \end{pmatrix}; \vec{y} = \begin{pmatrix} \ln Tr(M_1) \\ \ln Tr(M_2) \\ \cdots \\ \ln Tr(M_N) \end{pmatrix}.$$

3.3 Distribution of Stability Exponent

After the rays propagated, we calculated $\nu(t)$. For a given time t_1, we calculated ν using all the data points before time t_1 with Eq. (12). This was repeated several times to create a discrete function $\nu(t)$ for each ray.

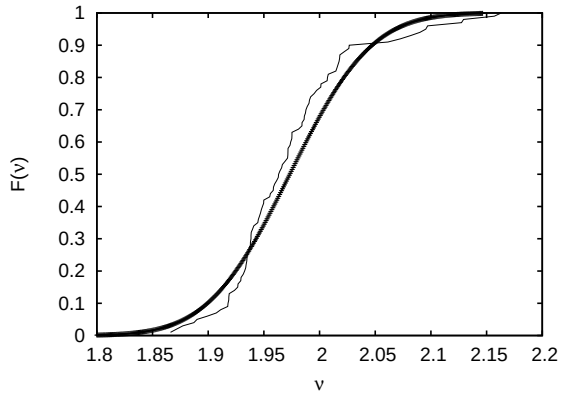

Figure 5: The heavy line is the curve fit to the data using Eq. (13). The lighter line is $\nu_{sort}(t)$ produced using 100 rays propagated to time $t = 50$ and Eq. (12).

Next, a time t_2 was selected and all the values for ν were collected from each ray's $\nu(t)$. These values were sorted increasingly to create $\nu_{sort}(t)$. Finally we plotted $\nu_{sort}(i)$ versus i/N where N is the total number of rays; refer to Fig. 3.3. This created a cumulative distribution which is a Gaussian distribution because the log of a product of random variables acts like a sum of random variables. The stability matrix should have the statistical properties of an ensemble of products of uncorrelated, random matrices. Thus, our distribution was fit to a curve using

$$F_\nu(x) \quad = \quad \frac{1}{2}\left(1 + erf\left[\frac{x - \langle\nu\rangle}{\sqrt{2\sigma_\nu^2}}\right]\right). \tag{13}$$

where $\langle\nu\rangle$ is the average value of ν and σ_ν^2 is the variance.

ACKNOWLEDGMENTS

We gratefully acknowledge the support for this research by the National Science Foundation's Research Experience for Undergraduates (REU) program under the grant PHY-0649023 and PHYS-0555301. We also thank Dr. Steven Tomsovic for his support and knowledge. Finally, we gratefully thank graduate student Katherine Hegewisch for her help, encouragement, valuable time, and input.

A Simulations

In order to follow the dynamics of the Tr(M) of each ray, fourth order Runge Kutta was coded to solve the 20 differential equations in Eq. (2) and Eq. (5).

At first, we utilized a fixed step process. The error is dependent on the chosen step size, which we set to 0.0001 with error equal to 0.0001^5. Although this error is very small, this process is very inefficent. First, the step size never changes, so during linear parts of the solution little steps were taken when larger steps would be more efficient. Second, if the step size is not small enough, vital parts of the solution could be missed. Finally, this process is very slow. In fact, to run 20 rays with 10,000 points each with a step size of 0.0001 it took nearly two hours. This was without calculating the elements of the stability matrix or the trace. The solver only needed to find the numerical solution to Eq. (2). A much faster process was needed.

Adaptive step size Runge Kutta changes the step size based on an error tolerance defined by the user. Using the Cash-Karp method of solving differential equations, the error in the solution is the difference between the fourth- and fifth- order solutions. This change in the program solved the three aformentioned problems. The program will take a larger step if the calculated error is low and a smaller step if the error is high. Furthermore, the code prevents the step size from getting so small that computer round-off causes

the step size to basically be zero. Even more beneficial is the drastic cut in computing time. Calculating the solution to six differential equations using 20 rays, finding the trace, and writing files took this program one hour whereas the fixed step would take approximately 7 hours.

For our study, we allowed the error tolerance ϵ to be 0.001. Starting the initial step size at $h = 0.0001$ and taking 10,000 adaptive steps could propagating the ray to x$\geq$200. Had the step size not been adaptive, the ray would end at x=1. Thus, the adaptive step size has significant advantages over the fixed step size only in part due to the significant decrease in computing time and increase in data collection.

B Calculating the random potential

Programming the potential in fortran is fairly easy. A function was created with a do-loop that calculates the value of Eq. (3) at a given x and y. The difficulty arises in creating the random $\theta_j s$ and $\phi_j s$. Random number generators created by computers are not truely random; the algorithm can be calculated and the results predicted. However, most programs come very close to creating truly random variables. The debate boils down to two issues: randomness and computing time. We needed a program that could create pseudo-random variables fairly quickly. Thus we sacrificed slightly more random variables for a cut in computing time. The program we chose comes with the computer and uses a seed to calculate a float between 0 and 1. The same seed will produce the same random variables.

References

[1] J. A. Colosi, E. K.Scheer, and S. M. Flatte et al. Comparisions of measured and predicted acoustic fluctuation for a 3250-km propagation experiment in the eastern north pacific ocean. *J. Acoust. Soc. Am*, 105:3202–3218, 1999.

[2] S. Tomsovic and M. G. Brown. Ocean acoustics: a novel laboratory for wave chaos.

[3] M. A. Topinka, B. J. Leroy, R. M. Westervelt, S. E. J. Shaw, R. Fleischmann, and E. J. Heller. Coherent branched flow in a two-dimensional electron gas. *Nature*, 410:183–186, 2001.

[4] M. A. Wolfson and S. Tomsovic. On the stability of long-range sound propagation through a structured ocean. *J. Acoust. Soc. Am*, 109:2693–2703, 2001.